International Journal of Automotive Technology, Vol. 7, No. 2, pp. 129–137 (2006)

1229–9138/2006/026–02

TRANSIENT FLAMELET MODELING FOR COMBUSTION PROCESSES OF HSDI DIESEL ENGINES

H. J. KIM[1], S. M. KANG[1], Y. M. KIM[1]*, J.-H. LEE[2] and J.-K. LEE[2]

[1]Department of Mechanical Engineering, Hanyang University, Seoul 133-791, Korea
[2]Hyundai Motor Company, 772-1 Jangduck-dong, Hwaseong-si, Gyeonggi 445-706, Korea

(Received 12 March 2005; Revised 19 October 2005)

ABSTRACT–The representative interactive flamelet (RIF) concept has been applied to numerically simulate the combustion processes and pollutant formation in the HSDI diesel engine. In order to account for the spatial inhomogeneity of the scalar dissipation rate, the eulerian particle flamelet model using the multiple flamelets has been employed. The vaporization effects on turbulence-chemistry interaction are included in the present RIF procedure. the results of numerical modeling using the rif concept are compared with experimental data and with numerical results of the widely-used ad-hoc combustion model. Numerical results indicate that the rif approach including the vaporization effect on turbulent spray combustion process successfully predicts the ignition delay characteristics as well as the pollutant formation in the HSDI diesel engines.

KEY WORDS : Auto-ignition, Fuel sprays, Vaporization effects, Representative interactive flamelet (RIF), Multiple flamelets, DI Diesel engine

1. INTRODUCTION

In comprehensively modeling the spray combustion processes (Chikahisa *et al.*, 2002) in DI diesel engines, numerical modeling of an auto-ignition process is quite important to correctly predict the combustion and pollutant formation characteristics. The Shell ignition model (Halstead *et al.*, 1975; Kong *et al.*, 1995; Sazhina and Sazhin, 2000) is generally used to simulate the spray ignition process. However, the Shell ignition model is unable to include the turbulent effects on the ignition process and it has the basic shortcoming that the parameters must be tuned according to the combustion conditions. In order to overcome this defect, Pitsch *et al.* (1996) suggested the Representative Interactive Flamelet (RIF) Model. This model does not require the tuning of parameters and it can account for the turbulence-chemistry interaction based on the detailed chemistry. Hence, auto-ignition, partially premixed burning, diffusive combustion and pollutants (NOx, soot) formation need not to be modeled individually. This transient flamelet model has the basic advantage to efficiently simulate the three-dimensional combustion processes of the internal combustion engines with the widely varying chemical and fluid dynamic time scales. Wan *et al.* (1997) predicted auto-ignition delay time and location using RIF model. (Pitsch and Peter, 1998) reduced the detailed kinetic reaction mechanism to 14-step mechanism and then studied auto-ignition process and relationship between auto-ignition delay time and scalar dissipation rate in detail. To account for the spatial inhomogeneity of the scalar dissipation rate in the spray flame field, Barths *et al.* (1998) devised the multiple flamelets procedure. Recently Kim *et al.* (2004) and Yu *et al.* (2001) numerically investigated the autoignition and flame propagation of gaseous and spray jets injected into a high-temperature and high-pressure by the multiple RIF model.

On the other hand, most of the previous works for simulation of spray combustion have neglected the effects of spray vaporization except the source term due to vaporization for mean mixture fraction. However, the recent DNS results by Reveillon and Vervisch (2000) revealed that the impact of vaporization sources on the small scales of the turbulent fuel distribution modifies significantly the fluctuations of mixture fraction and subsequently the scalar dissipation rate. Demoulin and Borghi (2000) also proposed the new model to include these major effects of spray vaporization on the mixture fraction fluctuations and the PDF model.

Our ongoing research is ultimately aiming at developing the reliable, stable and efficient combusion model which can realistically simulate the spray dynamics, vaporization, auto-ignition, combustion and pollutant

*Corresponding author. e-mail: ymkim@hanyang.ac.kr

formation process in DI diesel engine. In order to account for the vaporization effects on the mixture fraction fluctuations and the pdf model, the present study employs the model proposed by Demoulin and Borghi (2000). The coupling between complex chemistry and turbulence are treated by employing the Representative Interactive Flamelet (RIF) Model. In order to account for the spatial inhomogeneity of the scalar dissipation rate, the Eulerian Particle Flamelet Model using the multiple flamelets has been employed.

This study has been mainly motivated to critically evaluate the predicative capability of two combustion models including the Shell ignition/eddy dissipation model and the RIF model as well as to numerically investigate the vaporization effects on the turbulent spray combustion processes in the DI diesel engines. Since the cetane numbers of Diesel fuel (CN-50) and n-heptane (CN-56) that control the ignition delay times are quite close, numerical simulations for combustion processes of an n-heptane fueled DI Diesel engine have been carried out. All relevant physical submodels are implemented in the modified KIVA-3V code (Amsden, 1997). Computations are performed for four injection timings by using the Shell ignition/eddy dissipation model and the RIF model with and without the vaporization effects on the turbulent combustion. In addition to the RIF model, Eulerian Particle Flamelet model with the vaporization effect is carried out. In terms of ignition delay, cylinder pressure histories and pollutant emission, numerical results are compared with measurements for Cummins N-14 engine (Venkatesan and Abraham, 2000) and turbocharged HSDI diesel engine.

2.NUMERICAL AND PHYSICAL MODELS

All the gas-phase and liquid-phase processes are modeled by a system of unsteady, multi- dimensional equations. The gas-phase equation is written in an Eulerian coordinate whereas the liquid-phase is presented in Lagrangian coordinates. The two-way coupling between the two phases is described by the interaction source terms that represent the rates of momentum, mass and heat transfer. To realistically represent the physical processes involved in the spray dynamics, the present approach employs the hybrid breakup model (Beatrice *et al.*, 1996), the stochastic droplet tracking model (Kim *et al.*, 1994) and collision model (O'Rouke, 1981). In this study, two combustion models including the shell ignition/eddy-dissipation model and the RIF model are implemented in the KIVA-3V code (Amsden, 1997). In the present RIF approach, the modified formulations have been employed to account for the spray vaporization effects on the mixture fraction fluctuations and the pdf model. The main features of two combustion models are briefly described below.

2.1. Shell Ignition/Eddy-Dissipation Model

The Shell ignition model (Halstead *et al.*, 1975, Kong *et al.*, 1995, Sazhina and Sazhin, 2000) is generally used to simulate the spray ignition process. However, the Shell ignition model is unable to include the turbulent effects on the ignition process and it has the basic shortcoming that the parameters must be tuned according to the combustion conditions. This model also requires the solution of some species transport equations including semi-empirical chemical source terms in CFD calculation. Moreover, for simulating the high-temperature combustion processes after auto-ignition, the eddy-dissipation model (Magnussen and Hjertager, 1977) need to be turned on. In terms of the pollutant model, soot formation and oxidation have been modeled by using the Hiroyasu soot formation and Nale and Strickland-Constable oxidation models, respectively (Patterson *et al.*, 1994). For NO, the extended Zeldovich mechanism has been used to estimate the thermal NOx. This model is incapable of predicting the prompt and fuel NOx contribution. The ad-hoc correction factor is usually used to convert NO predictions to NOx estimation.

2.2. RIF-based Combustion Model

In the Representative Interactive Flamelet (RIF) model, the turbulent flow field can be calculated with a Computational Fluid Dynamics (CFD) code and the laminar flamelet equations can be solved with a flamelet code. However the flamelet equations (Peters, 1984) are solved in a separate code, interactively coupled with a main code. Flamelet parameters obtained from the main code are used for calculating flamelet equations, and then species mass fractions gained from flamelet code are passed to the main code.

Two additional transport equations for the local mean mixture fraction $\tilde{Z}$ and its variance $\tilde{Z}''^2$ have to be solved in the CFD code to define the local mean species composition. So far, most of the turbulent combustion models originally developed for gaseous flames have been applied to simulate the spray combustion processes without considering the vaporization effects on the small-scale turbulent mixing and the turbulent combustion. In order to account for the vaporization effects on the turbulent spray combustion, the present study adopts the model proposed by Demoulin and Borghi(2000). The transport equation of mixture fraction variance is derived by using the pdf transport equation for mixture fraction. The equations for the mean mixture fraction $\tilde{Z}$ and its variance $\tilde{Z}''^2$ coupled with the vaporization effects can be written as follows:

$$\frac{\partial}{\partial t}(\bar{\rho}\tilde{Z})+\frac{\partial}{\partial x_j}(\bar{\rho}\tilde{u}_j\tilde{Z})=\frac{\partial}{\partial x_j}\left(\frac{\mu_t}{\sigma_Z}\frac{\partial\tilde{Z}}{\partial x_j}\right)+\bar{\rho}\tilde{\omega}_v \tag{1}$$

$$\frac{\partial}{\partial t}(\bar{\rho}\tilde{Z}''^2)+\frac{\partial}{\partial x_j}(\bar{\rho}\tilde{u}_j\tilde{Z}''^2)=\frac{\partial}{\partial x_j}\left(\frac{\mu_t}{\sigma_{Z''^2}}\frac{\partial\tilde{Z}''^2}{\partial x_j}\right)+\frac{2\mu_t}{\sigma_{Z''^2}}\frac{\partial^2\tilde{Z}}{\partial x_j^2}-\bar{\rho}\tilde{\chi} +2(\bar{\rho}\widetilde{Z\omega}_v-\bar{\rho}\tilde{Z}\tilde{\omega}_v)+\bar{\rho}\widetilde{Z^2}\tilde{\omega}_v-\bar{\rho}\widetilde{Z^2\omega}_v \tag{2}$$

The last four additional source terms appeared in (5) account for the vaporization effects on mixture fraction variance. These new correlations taking into account the fluctuation of equivalence ratio due to vaporization are in an unclosed form. By assuming that the spray vaporization takes places only at the liquid surface, Demoulin and Borghi (2000) have proposed the model for these correlations:

$$\bar{\rho}\widetilde{Z\omega}_v\approx\bar{\rho}\widetilde{Z_s\omega}_v=\sum_p Z_s^p\frac{\dot{m}_p}{V} \tag{3}$$

and

$$\bar{\rho}\widetilde{Z^2\omega}_v\approx\bar{\rho}\widetilde{Z_s^2\omega}_v=\sum_p (Z_s^p)^2\frac{\dot{m}_p}{V} \tag{4}$$

where the subscript s denotes the value at the liquid surface. These additional source terms are mainly contributed to the production of mixture fraction fluctuations. In spray combustion processes, these terms are contributed to increase the scalar dissipation rate and the ignition delay time as well as to modify the small-scale mixing processes and the spray structure.

Another important effect due to vaporization is related to the fact that the upper limit of mixture fraction is not unity in spray combustion processes. Therefore, the upper limit (Z_{ini}) of mixture has to be determined. By utilizing the conditional pdf of Z_{ini} and mixture fraction equation, Demoulin and Borghi (2000) derived the following balance equation.

$$\frac{\partial}{\partial t}(\bar{\rho}\,\tilde{Z}\,\bar{Z}_{ini})+\frac{\partial}{\partial x_j}(\bar{\rho}\,\tilde{u}_j\,\tilde{Z}\,\bar{Z}_{ini})= \frac{\partial}{\partial x_j}\left(\frac{\mu_t}{\sigma_Z}\frac{\partial\tilde{Z}\,\bar{Z}_{ini}}{\partial x_j}\right)+\bar{\rho}\int_0^1 Z_{ini}\,\omega_{v|Z_{ini}}\,dZ_{ini} \tag{5}$$

For a given position, therefore, the allowable space for mixture fraction Z has to be automatically adjusted from 0 to $\bar{Z}_{ini}$. In the present study, the β-pdf $\tilde{P}(Z;\tilde{x},t)$ is employed and its shape has been renormalized from the three constraints:

$$1=\int_0^{\bar{Z}_{ini}}\tilde{P}(Z)dZ,\quad \tilde{Z}=\int_0^{\bar{Z}_{ini}}Z\tilde{P}(Z)dZ, \quad \tilde{Z}''^2=\int_0^{\bar{Z}_{ini}}(Z-\tilde{Z})^2\tilde{P}(Z)dZ \tag{6}$$

This modified upper limit of mixture fraction also influences the ignition delay and the spray combustion processes. Decease in the upper limit mixture fraction is contributed to increase the probability of combustion in a given mixture fraction.

In order to account for the spatial inhomogeneity of scalar dissipation rate, the present study employs the Eulerian Particle Flamelet Model (EPFM) by Barths *et al.* (1998) utilizing the multiple RIFs. In this multiple RIF approach, each cell of domain is not belong to one flamelet but belong to several flamelets. Thus the local species mass fractions can be determined by considering the distribution of multiple flamelets. Scalar dissipation rate for each flamelet is based on a surface averaged value at stoichiometric mixture and it can be calculated by convert-ing the surface integrals into volume integrals. The detailed formulation of the present multiple RIF model can be found elsewhere (Barths *et al.*, 1998, Kim *et al.*, 2004; Yu *et al.*, 2001).

Unlike the shell ignition/eddy dissipation model, the RIF concept has the capabilities to realistically predict the detailed soot formation process, NOx formation including thermal NO path, prompt and nitrous NOx formation, and reburning process by hydrocarbon radical without any ad-hoc procedure as well as the main turbulent combustion processes. The detailed chemical mechanism of heptane used in this study comprises 114 elementary reactions with 43 species for n-heptane and 101 irreversible reactions with 13 additional species related to NOx formation. This reaction scheme includes fuel oxidation, low temperature degenerate chain branching to describe auto-ignition, and a reaction mechanism for NOx formation, including thermal, prompt, nitrous NOx and reburn by hydrocarbon radicals. In order to estimate the soot emission, this study employs the soot formation model proposed by Moss *et al.* (1995) This model is required to solve the following two transport equations for the volume fraction and number density of soot. In the present RIF-based approach, the laminar flamelet data obtained from OPPDIF are used to express the source terms appearing in two transport equations of soot volume fraction and number density as a function of the mixture fraction Z. By convoluting these source terms with PDF, the mixture fraction averaged source terms are obtained.

3. RESULTS AND DISCUSSION

The Representative Interactive Flamelet (RIF) concept has been applied to numerically simulate the combustion processes and pollutant formation in the direct injection diesel engine. Based on numerical results for Cummins N-14 engine and turbocharged HSDI diesel engine, the detailed discussions have been made below.

3.1. Cummins N-14 Engine

The RIF-based turbulent combustion models and the Shell ignition/ eddy dissipation model have been applied to simulate the spray dynamics, vaporization, auto-ignition, combustion process and pollutant (NOx, soot) formation in the DI diesel engine. We have chosen the validation case as the experimental results (Venkatesan and Abraham, 2000) for Cummins N-14 engine. The engine specification and computational conditions are given in Table 1 and 2.

Computation starts at bottom dead center (BDC) and continues until the exhaust valve opens at 130°CA. In experiments, a diesel fuel is used. Since the detailed chemical kinetics of diesel fuel are still uncertain, n-heptane is used as a fuel in numerical simulation. The orifice diameter is 200 microns and a spray angle is 14°. Computations are performed for 45° sector of combustion chamber. Numerical results are compared with the experimental data of Prasanna *et al.* (Venkatesan and Abraham, 2000).

For simplicity of presentation, Model 1, Model 2, Model 3 and Model 4 are used to represent the the Shell ignition/eddy dissipation model, the RIF model, the RIF model and the Eulerian Particle Flamelet model including vaporization effects on turbulent combustion. In Figure 1(a), the simulated cylinder pressure histories obtained by Model 1 are compared with the measured data for 4 injection timings. For the injection timing near TDC, computed results are well agreed with experimental data. By continuously retarding the injection timing, the agreement between prediction andmeasurement becomes much worse. The largest deviations in ignition delay time and pressure histories are corresponding to the latest

Table 1. Engine specification of Cummins N-14 DI diesel engine.

Engine type	Cummins N-14
Bore (cm)	13.97
Stroke (cm)	15.24
Squish (cm)	0.378
Compression ratio	16.5
Diplacement volume (cm^3)	2340
Connecting rod length (cm)	30.48
Injection nozzles	8
Injector hole diameter (cm)	0.02
Spray inclination angle (deg)	76

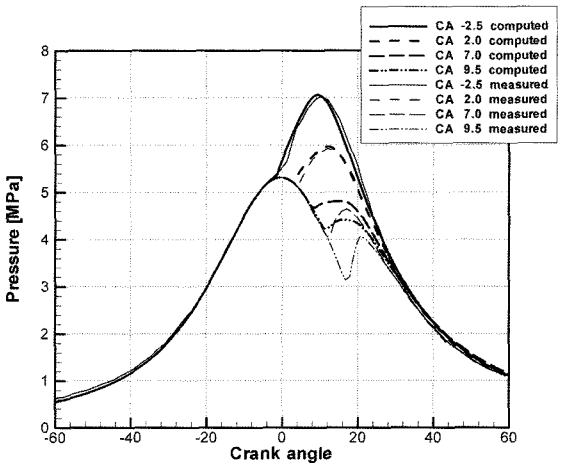

(a) Model 1

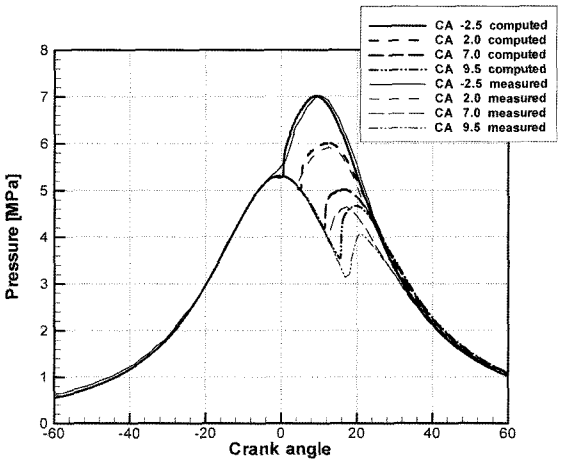

(b) Model 2

Figure 1. Cylinder pressure histories for 4 injection timings.

Table 2. Computational conditions.

Case	Computation sector (°)	RPM	Initial air pressure (MPa)	Initial air temp. (K)	Mass of air (g)	Mass of fuel (g)	Wall temp. (K)	SOI (°CA)	EOI (°CA)
A	45	1200	0.1244	408	2.627	0.0657	400	–2.5	4.5
B	45	1200	0.1244	408	2.627	0.0657	400	2	10
C	45	1200	0.1244	408	2.627	0.0657	400	7	15
D	45	1200	0.1244	408	2.627	0.0657	400	9.5	17.5

injection timing (9.5 CA). For the relatively late injection timings (7 and 9.5 CA) where the nonequlibrium chemistry effects are dominant due to the relatively low chamber temperature and intense turbulence associated with the high-speed injection, the Shell ignition/eddy dissipation model substantially underestimates the ignition delay time and predicts the quantitatively and qualitatively wrong pressure histories. These discrep cies could be related to the defect of the Shell ignition/eddy dissipation model (Model 1) which is unable to properly account for the turbulence-chemistry interaction. These numerical results suggest that the Shell ignitiong/eddy dissipation model can not be applicable to simulate the combustion processes of DI diesel engine with the far retarded injection. In Figure 1(b), the simulated cylinder pressure histories obtained by the RIF model (Model 2) are compared with the measured data for 4 injection timings. The computed and measured pressure histories and ignition delay times have the reasonably good agreement for all cases. Even if the agreement in the relatively late injection timings (7 and 9.5 CA) has been considerably improved in comparison with the Shell ignition/eddy dissipation model, the underestimation of ignition delay time and overestimation of cylinder pressure are quite noticeable for the relatively late injection timings (7 and 9.5 CA). These discrepancies could be mainly related to the vaporization effects on the turbulent combustion process and the spatial inhomogeneity of scalar dissipation rate in the transient spray flame field.

In order to improve the predicted ignition delay time and cylinder pressure histories, the single RIF model (Model 3) and multiple RIF model (Model 4) including vaporization effects on turbulent combustion process is used to simulate the spray combustion processes for two injection timings (2 CA and 7 CA). This multiple RIF approach adopts lthe Eulerian Particle Flamelet model utilizing 10 RIFs which is capable of accounting for spatial inhomogeneity of the scalar dissipation rate. Figure 2 displays the simulated cylinder pressure histories obtained by Model 3 and Model 4, and the measured data for 2 injection timings (2.0 CA, 7.0 CA). When the vaporization effects on turbulent combustion model are included in the single RIF approach, it can be clearly seen that the agreement in the predicted and measured ignition delay times has been significantly improved especially for the relatively late injection timing (7 CA). These numerical results indicate that the vaporization effects on turbulent combustion process play a crucial role in the relatively late injection timing with the much lower cylinder temperature and pressure. However, in terms of the cylinder pressure histories, the present model noticeably overestimate the cylinder pressure after autoignition at the relatively late injection timing (7 CA). In conjunction with the single RIF model, neglect of the

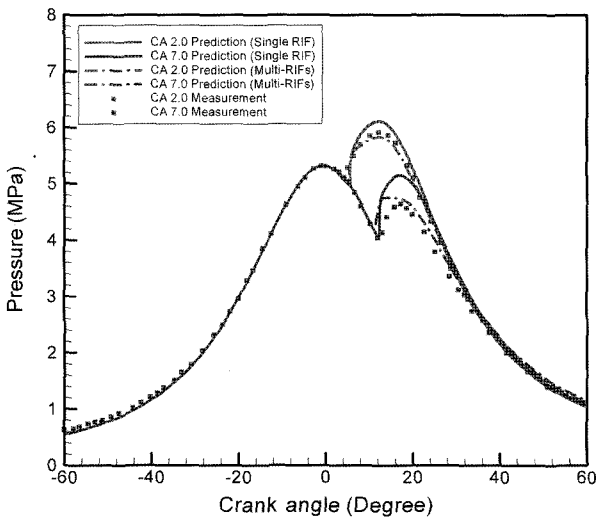

Figure 2. Cylinder pressure histories for 4 injection timings (Model 3 & Model 4).

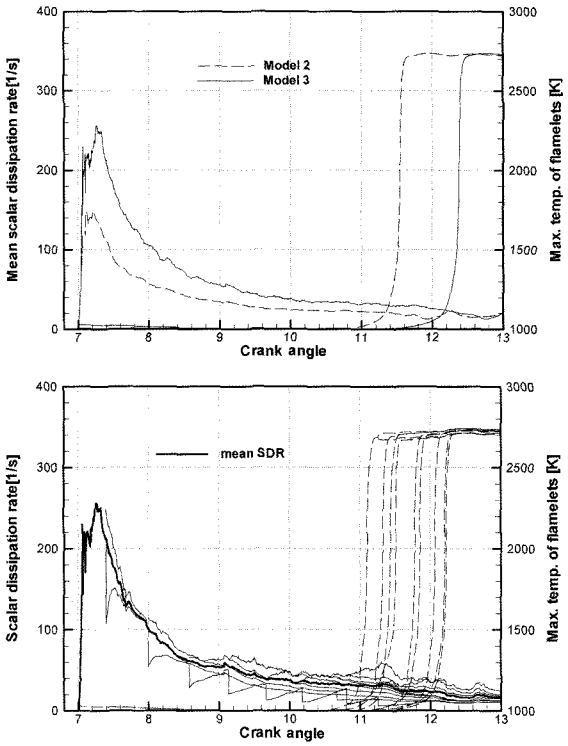

Figure 3. Temporal evolution of the scalar dissipation rates and the maximum temperature for ignition timings at 7° CA (a) Model 2 & Model 3, (b) model 4.

spatial inhomogeneity of scalar dissipation rate is partially responsible for the overprediction of cylinder pressure. When the spatial inhomogeneity of scalar dissipation rate and the vaporization effects on turbulent combustion model are included in the EPFM approach,

the predicted cylinder pressure history is reasonably well agreed experimental data, compared to the single RIF approach (Model 3). However, Model 4 predict the earlier autoignition than does Model 3. Figure 3(a) shows the temporal evolutions of the scalar dissipation rate and mean temperature predicted by Model 2 and Model 3. At the initial stage of liquid fuel injection, the scalar dissipation rate rapidly increases and reaches to a peak value due to the high vaporization rate and the intense turbulence generated by the high-velocity injection process. The high injection velocity enhances the liquid jet disintegration, droplet breakup, interphase convective heat transfer, droplet vaporization and gas-phase turbulence. Particularly, the droplet vaporization rate is greatly increased by reducing the vaporization characteristic time in the strong droplet breakup process as well as by increasing the interphase convective heat transfer. As a result, this high injection velocity abruptly increases the scalar dissipation rate by elevating these nonequilibrium effects such as the enhanced turbulence, the high spray evaporation rate and the large gradient of mixture fraction. Shortly after this initial injection period, the scalar dissipation rate gradually decreases to the slow-varying low value since the fuel vapor spreads out the ambient flow field and the turbulence is continuously dissipated. At the small scalar dissipation rates, the diffusive losses become so small that heat and radicals produced by the chemical reaction are continuously increased and the mixture field can be finally ignited. Compared to the RIF model (Model 2), the RIF model with vaporization effect (Model 3) predicts the much higher level of the averaged conditional scalar dissipation rate. This trend directly reflects the spray vaporization characteristics predicted by these models. Therefore, when the vaporization effects are coupled with the RIF turbulent combustion model, the averaged scalar dissipation rate considerably increases due to the increased production of mixture fraction fluctuations. These numerical results suggests that the vaporization effects coupled with the turbulent combustion models could be progressively influencing to the auto-ignition process and the spray combustion processes in the relatively retarded injection operation of DI diesel engines. Figure 3(b) presents the temporal evolutions of the scalar dissipation rate and maximum temperature for 10 flamelets predicted by the EPFM approach (Model 4). In context with this EPFM model, the calculation starts with a single flamelet and the first flamelet is split into two such that one of them represents the larger and the other does the lower values of the scalar dissipation rate. Since this splitting process continues, it is quite possible that one of the flamelets can be ignited with a relatively low scalar dissipation rate. This is the main reason for the earlier ignition predicted by Model 4.

3.2. Turbocharged HSDI Diesel Engine

Experimental results for the turbocharged HSDI diesel engine have been chosen as the second validation case. The engine specification and initial conditions are given in Table 3 and 4. Computation starts at bottom dead center (BDC) and continues until the exhaust valve opens at 130°CA. In this case, n-heptane is also used to simulate a diesel fuel. The orifice diameter is 168 microns and a spray angle is 12°. Computations are performed for 72° sector of combustion chamber. Based on the measured initial swirl number, 2.0, the corresponding initial flow-field is generated. The instantaneous fuel flowrate for the

Table 3. Engine specification of turbocharged HSDI diesel engine.

Engine type	Turbocharged HSDI engine
Bore (cm)	8.3
Stroke (cm)	9.2
Compression ratio	17.7
Displacement volume (cm^3)	498
Injection nozzles	5
Injector hole diameter (cm)	0.0168
Spray inclination angle (deg)	75

Table 4. Initial and injection condition for turbocharged HSDI diesel engine.

	RPM	Pi (Mpa)	Ti (K)	Mass of fuel (mg)	SOI (°CA)	EOI (°CA)
Case	2000	0.245	420	47.77	−33.2	15.8

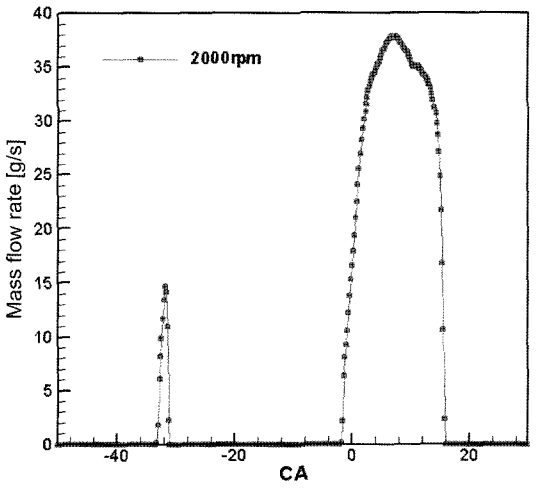

Figure 4. fuel mass flow rate for turbocharged HSDI diesel engine.

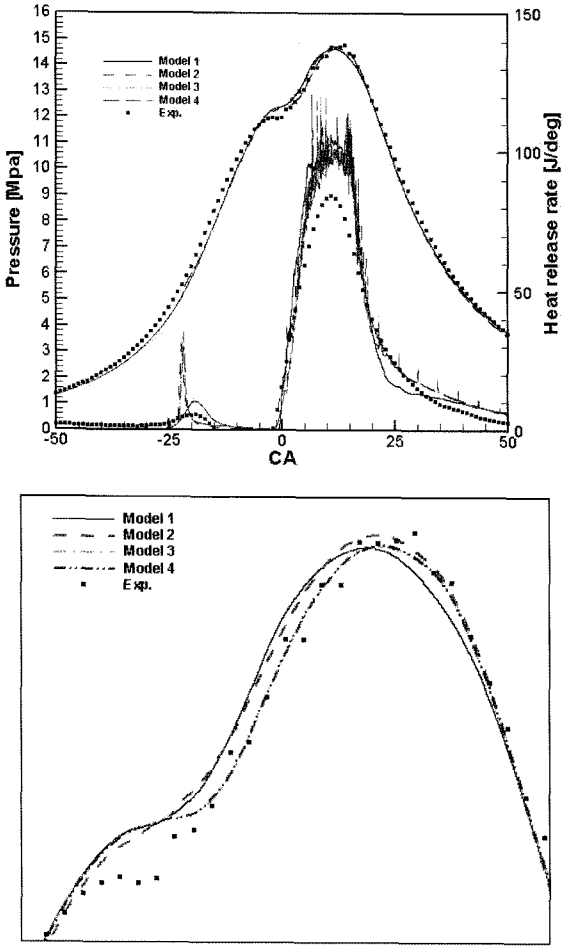

Figure 5. Cylinder pressure histories and Heat release rate for four models.

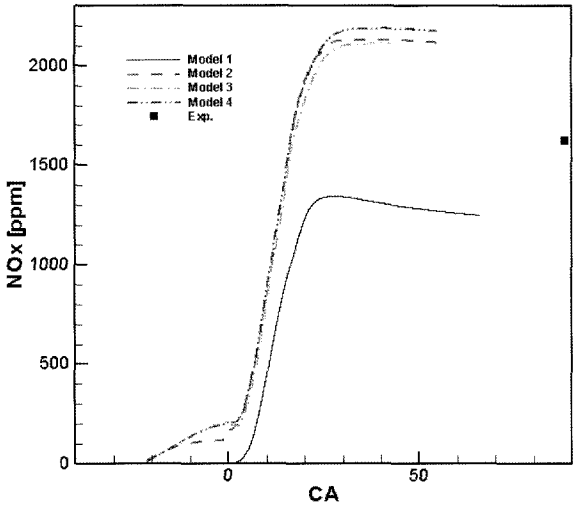

Figure 6. NOx emission for four models.

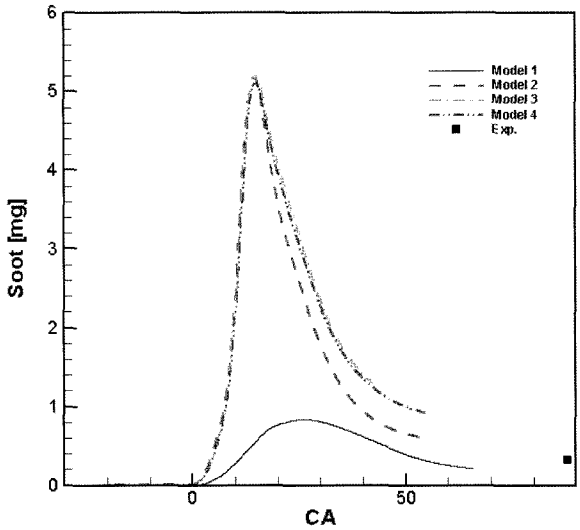

Figure 7. Soot emission for four models.

pilot injection and main injection are plotted in Figure 4. In Figure 5, the simulated cylinder pressure histories obtained by the Shell ignition/eddy dissipation model (Model 1) and the RIF-based model (Model 2-4) are compared with the measured cylinder pressure and heat release rate. If we closely take a look at numerical results, compared to Model 2, Model 1 predicts the slightly longer ignition delay and the slightly lower peak cylinder pressure. When the vaporization effects (Model 3 and 4) on the turbulent combustion model are included, the cylinder pressure noticeably decreases especially shortly after the main injection and the conformity with the measure cylinder pressure has been improved. As shown in numerical results, Model 4 predicts the nearly identical pressure obtained by Model 3. These numerical results indicate that the spatially inhomogeneous effect of scalar dissipation rate (Model 4) is not quite important especially for this operation condition of the turbocharged high-speed multiple injection diesel engine which has the rapid atomization and air-fuel mixing process. In the overall comparison with the measure cylinder pressure and heat release rate, computed results obtained by four models have a good agreement with measurements. However, around at the main injection stage, two models over-estimate the cylinder pressure and there also exists qualitatively different trend between prediction and measurement. In measurement, at the short period just after the main injection, the cylinder pressure is nearly constant or even very slightly decreases and then abruptly increases. This phenomenon could be directly related to the flame quenching due to the cooling effect as well as the local extinction and reignition in the lifted flame zone of the very high scalar dissipation rate. These two effects might be caused by the extremely high scalar dissipation and evaporation in the high-speed injection and high-

pressure condition (120 atm) of the turbocharged HSDI engine. When the vaporization effects (Model 3 and 4) on the turbulent combustion model are included, numerical results clearly indicate the qualitatively improved conformity with the measure cylinder pressure shortly after the main injection. In order to correctly capture this complex turbulent spray combustion processes, the comprehensive model must have the prediction capability to realistically represent the high-pressure and supercritical evaporation as well as the turbulent partially premixed lifted flame accompanied with local extinction and reignition. This could be the very challenging task in the turbulent spray combustion modeling.

Figures 6 and 7 present the measured and predicted NOx and soot emission characteristics in the turbocharged HSDI diesel engine. Compared to the measured NOx emission level, the Shell ignition/eddy dissipation model (Model 1) underestimates the NOx emission and three RIF-based model (Model 2, 3, 4) overestimate the NOx level. As mention earlier, the Shell ignition/eddy dissipation model (Model 1) calculates the thermal NOx by utilizing the equilibrium concentration of O radical which is much lower than superequilibrium radical concentration in the turbulent flamefield. Thus, to estimate the NOx emission level, Model 1 requires the ad-hoc tuning constant and it can not be the general-purpose prediction tool. The overestimated NOx level in the RIF-based models could be attributed to the neglect of radiation, use of n-heptane to simulate diesel fuel, and the defects of the present turbulent combustion model. Compared to the RIF-based models, the Shell ignition/ eddy dissipation model (Model 1) is unable to predict the NOx formation shortly after the pilot injection. Since Model 1 extremely underestimate the O radical concentration and is unable to predict the prompt NOx, fuel NOx, and hydrocarbon-radical induced reburn chemistry, Model 1 predicts the nearly zero NOx emission after the pilot injection.

In terms of the soot emission level, the RIF-based combustion models (Model 2, Model 3 and Model 4) predict the reasonably good agreement with the measured soot emission level while the Shell ignition/eddy dissipation model underestimate the soot emission level. There exists the distinctly different trend in the soot formation and oxidation processes because the Shell ignition/eddy dissipation model (Model 1) and the RIF-based combustion models (Model 2, 3, 4) use the different soot model. Compared to Model 1, the RIF-based combustion models (Model 2, 3, 4) utilizing the more realistic soot model predict the rapid soot formation and oxidation processes. In the RIF-based models, the rapid soot formation results from the fuel-rich high-temperature zone and the rapid soot oxidation is caused by the relatively high OH concentration created in the hot combustion zone. When the vaporization effects (Model 3 and 4) on the turbulent combustion model are included, the soot oxidation rate in the late combustion period is relative slow down due to the relatively low OH level predicted by Model 3 and 4. The rapid soot formation rate in the RIF model could be partially responsible for the use of n-heptane to simulate diesel fuel, the neglect of radiation, and the defects of the present turbulent combustion model.

4. CONCLUSIONS

The RIF-based turbulent combustion model and the Shell ignition/eddy dissipation model have been applied to simulate the spray dynamics, vaporization, auto-ignition and combustion process in the Cummins N-14 DI diesel engine and turbocharged HSDI diesel engine. Based on numerical results, the following conclusion can be drawn.

(1) Numerical results indicate that the RIF-based model including the vaporization effects on turbulent combustion process is capable of predicting auto-ignition and spray combustion processes in the wide range of injection timings in the DI diesel engines.

(2) In case of the Cummins N-14 DI diesel engine, for the relatively late injection timings (7 and 9.5 CA) where the nonequlibrium chemistry effects are dominant due to the relatively low chamber temperature, the Shell ignition/eddy dissipation model substantially underestimate the ignition delay time and predict the quantitatively and qualitatively wrong pressure histories.

(3) These numerical results indicate that the spatial inhomogeneity effect of scalar dissipation rate (Model 4) is relatively not important especially for the turbocharged high-speed mutiple direct-injection diesel engine which has the rapid atomization and air-fuel mixing process.

(4) In the overall comparison with the measure cylinder pressure and heat release rate of the turbochargred HSDI diesel engine, computed results obtained by four models have a good agreement with measurements. However, around at the main injection stage, all models overestimate the cylinder pressure and there also exists qualitatively different trend between prediction and measurement. When the vaporization effects (Model 3 and 4) on the turbulent combustion model are included, numerical results clearly indicate the qualitatively improved conformity with the measure cylinder pressure shortly after the main injection

(5) Compared to the measured NOx emission level, the Shell ignition/eddy dissipation model (Model 1) underestimates the NOx emission and three RIF-based model (Model 2, 3, 4) overestimate the NOx level. In terms of the soot emission level, the RIF-based combustion models predict the reasonably

good agreement with the measured soot emission level while the Shell ignition/eddy dissipation model underestimate the soot emission level.

(6) The discrepancies in the cylinder pressure and pollutant (NOx, Soot) emission might be attributed to the neglect of radiation, use of n-heptane to simulate diesel fuel, and the defects of the present RIF-based turbulent combustion model.

ACKNOWLEDGMENTS–This work was supported by Korea Research Foundation Grant (KRF-2005-042-D00020).

REFERENCES

Amsden, A. A. (1997). *A Block-Structured KIVA Program for Engines with Vertical or Canted Valves.* Los Alamos National Laboratory Report, LA-13313-MS.

Barths, H., Antoni, C. and Peters, N. (1998). Three-dimensional simulation of pollutant formation in a DI diesel engine using multiple interactive flamelets. *SAE Paper No.* 982459.

Beatrice, C., Belardini, P. and Bertoli, C. (1996). Cameretti, M., C., Cirillo, N., Fuel jet models for multidimensional diesel combustion calculation: an update. *SAE Trans.* **104**, **3**, 194–204.

Demoulin, F. X. and Borghi, R. (2000). Assumed PDF modeling of turbulent spray combustion. *Combustion Science and Technology*, **158**, 249–272.

Halstead, M. P., Kirsch, L. J., Prothero, A. and Quinn, C. P. (1975). A mathematical model for hydrocarbon auto-ignition at high pressures. *Proc. R. Soc. Lond., A.* **346**, 515–538.

Kong, S. C., Han, Z. and Reitz, R. D. (1995). The development and application of a diesel ignition and combustion model for multidimensional engine simulations. *SAE Paper No.* 950278.

Kim, S. K., Yu, Y., Ahn, J. and Kim, Y. (2004). Numerical investigation of the autoignition of turbulent gaseous jets in a high-pressure environment using the multiple-RIF model. *Fuel,* **83**, 375–386.

Kim, Y. M., Shang, H. M. and Chen, C. P. (1994). Studies on droplet-turbulence interactions. *KSME J.* **8**, **4**, 364–374.

Magnussen, B. F. and Hjertager, B. H. (1977). On mathematical modeling of turbulent combustion with special emphasis on soot formation and combustion. 16th *Symp. (Int.) Combustion,* 719–729.

Moss, J. B., Stewart, C. D. and Young, K. J. (1995). Modeling soot formation and burnout in a high temperature laminar diffusion flame burning under oxygen-enriched conditions. *Combustion and Flame,* **101**, 491–500.

O'Rouke, P. J. (1981). *Collective Drop Effects on Vaporizing Liquid Spray.* Los Alamos National Laboratory. Technical Report LA-9069-T.

Patterson, M. A., Kong, S. C., Hampson, G. J. and Reitz, R. D. (1994). Modeling the effects of fuel injection characteristics on diesel engine soot and NOx emissions. *SAE Paper No.* 940523.

Peters, N. (1984). Laminar diffusion flamelet models in non-premixed turbulent combustion. *Progress in Energy and Combustion Science* **10**, **3**, 319–339.

Pitsch, H., Barths, H. and Peters, N. (1996). Three-dimensional modeling of NO_x and soot formation in DI-diesel engines using detailed chemistry based on the interactive flamelet approach. *SAE Trans.* **105**, **4**, 2010–2024.

Pitsch, H. and Peters, N. (1998). Investigation of the ignition process of sprays under diesel conditions using reduced n-heptane chemistry. *SAE Paper No.* 982464.

Reveillon, J. and Vervisch, L. (2000). Spray vaporization in nonpremixed turbulent combustion modeling: a single droplet model. *Combustion and Flame,* **121**, 75–90.

Sazhina, E. M. and Sazhin, S. S. Heikal, M. R., Babushok, V. I. and Johns, R. J. R. (2000). A detailed modeling of the spray ignition process in diesel engines. *Combustion Science and Technology*, **160**, 317–344.

Chikahisa, T., Hishinuma, Y. and Ushida, H. (2002). Mixing conditions with spray-jet interaction for effective soot reduction in diesel combustion. *Int. J. Automotive Technology* **3**, **1**, 17–25.

Venkatesan, C. P. and Abraham, J. (2000). An investigation of the dependence of NO and soot emissions from a diesel engine on heat release rate characteristics. *SAE Paper No.* 2000-01-0509.

Wan, Y. P., Pitsch, H. and Peters, N. (1997). Simulation of autoignitton delay and location of fuel sprays under diesel-engine relevant conditions. *SAE Trans.* **106**, **3**, 1611–1621.

Yu, Y., Kim, S. K. and Kim, Y. (2001). Numerical modeling for autoignition and combustion processes of fuel sprays in high-pressure environment. *Combustion Science and Technology*, **168**, 85–112.